



Original scientific paper

Effect of nano yttria stabilized zirconia on corrosion behaviour of chromium oxide coatings on boiler steel

Khushdeep Goyal^{1,✉} and Rakesh Bhatia²

¹Department of Mechanical Engineering, Punjabi University, Patiala, India

²Yadavindra Department of Engineering, Punjabi University Guru Kashi Campus, Damdama Sahib, India

Corresponding author: ✉ khushgoyal@yahoo.com

Received: October 26, 2023; Accepted: November 23, 2023; Published: December 1, 2023

Abstract

In this research work, 5 wt.% nano yttria-stabilized zirconia (YSZ) reinforced chromium oxide-based nanocomposite coatings were prepared and successfully deposited on ASME-SA213-T-22 (T22) boiler tube steel substrates using high-velocity oxyfuel (HVOF) thermal spraying method. The corrosion behaviour of composite coating has been compared with that of conventional chromium oxide coating. All the coatings were analysed by scanning electron microscope, energy-dispersive X-ray spectroscopy and X-ray diffraction. It was found that the addition of 5 wt.% YSZ in the Cr₂O₃ matrix results in the reduction of the porosity of the coating and an increase in hardness. During corrosion investigations, it was found that YSZ-reinforced Cr₂O₃ nanocomposite coating on T22 provides better corrosion resistance than conventional Cr₂O₃ coating in the molten salt environment at 900 °C. The inclusion of YSZ has reduced porosity by filling in the gaps in the chromium oxide coating, causing particle interlocking, and preventing the entry of corroding species.

Keywords

Boiler steel tube; thermally sprayed coatings; chromium (III) oxide; zirconia ceramic; porosity, hardness

Introduction

Material conservation is becoming increasingly important due to the demands of the current and future global economy [1]. For many high-temperature aggressive environment applications, including boilers, internal combustion engines, gas turbines and industrial waste incinerators, degradation of metals and alloys due to hot corrosion or erosion has been identified as a serious problem [2]. Eventually, this means that repairing the damaged parts will be a difficult and expensive task. In light of this, any method for extending the component life would be highly desirable to all engineers and result in big financial savings. Corrosion is a pervasive issue that is still very relevant in a variety of industrial applications and products [3]. It causes component and system degradation

and eventual failure. In addition to the indirect expenses associated with shutdowns and lost productivity, billions of dollars are spent annually replacing corroded parts and equipment [4,5]. These components might malfunction prematurely and cause harm to people or even cause fatalities. The direct cost of corrosion in the United States and the European Union is projected to be between three and five percent of the member states GDP [6,7].

According to Sidhu and Prakash [8], hot corrosion and erosion account for more than 50 % of boiler tube failures in thermal power plants. Coal combustion produces extremely caustic chemicals deposited on the boiler tubes. Sulphur and oxygen combine to form SO₂, which then oxidizes to form SO₃. Na₂SO₄ is created when the SO₃, water vapour, and NaCl combine. When fuel containing vanadium is exposed to prolonged heat beyond its melting point of 550 °C, it oxidizes to produce V₂O₅, which then reacts with Na₂SO₄ to make sodium vanadates, which are extremely corrosive and low melting point compounds [7,9,10].

It has been found that applying protective coatings by thermal spraying works well and doesn't change the other characteristics of the base material [11]. One popular family of hard-facing procedures is thermal spraying, which differs from other processes in that it allows for almost minimal substrate dissolving, low substrate heat input, and freedom in choosing the coating material. Thermally sprayed coatings, which had limited value as corrosion protection coatings due to the presence of interconnected porosity in the structure, have gained popularity and have been thoroughly studied for corrosion-resistant properties since the introduction of the high-velocity oxyfuel spray (HVOF) technique. HVOF coatings provide strong, homogenous, low-porosity structures sufficiently thick to prevent electrolyte advancement [12-14]. The low flame temperature restricts the coating's ability to decompose and produce grains, while its hypersonic velocity speeds up the interaction between the powder and flame. Applying coatings to industrial installations on-site is made easier and more convenient by the continuous nature of the HVOF process [14,15].

In order to improve the qualities of boiler steels, several researchers have recently developed a variety of coatings using thermal spraying techniques. The thermal spraying approach creates porous coatings with several little microcracks or holes in them. *Via* these pores and microcracks, corrosive liquids and chemicals attack the substrate steels. Thus, there is still room for development of mechanical and microstructural qualities of these coatings. Many authors have reported the development of Cr₂O₃ coatings on steel alloys, but literature related to nano yttria-stabilized zirconia (Y₂O₃/ZrO₂) (YSZ) reinforced composite coatings is very limited. Therefore, there is scope to develop new nano yttria-stabilized zirconia (YSZ) mixed Cr₂O₃ nanocomposite coatings and to investigate the microstructure, porosity and microhardness of these newly developed composite coatings on boiler tube steel.

Experimental

Substrate material

Table 1 displays the nominal and measured compositions of T22 steel. The boiler tube was used to create the samples, which measured 22×15×5 mm.

Table 1. Chemical composition of T-22 steel (in weight percentage)

Composition	Content, wt.%									
	C	Mn	Si	S	P	Cr	Mo	V	Ni	Fe
Nominal	0.15	0.3-0.6	0.5-1	0.03	0.03	1.9-2.6	0.87-1.1	-	-	Balance
Actual	0.14	0.42	0.64	0.04	0.03	2.14	0.98	0.02	0.02	Bal.

The cut pieces were polished using silicon carbide paper. The samples were shot blasted with grit 45 alumina powder prior to applying various coatings.

Formulation of coatings

Using low energy ball milling, commercially available Cr_2O_3 powder was combined with five weight percent YSZ to create nanocomposite coating powder. In order to make Cr_2O_3 mixed with 5 wt.% YSZ ($\text{Y}_2\text{O}_3/\text{ZrO}_2$), 950 g of Cr_2O_3 and 50 g of YSZ were mixed. The blended powders were continuously rolled at 200 rpm for four hours.

Using the HVOF method, T22 boiler steel substrates were coated with different powders at Metallizing Equipment Company Limited in Jodhpur, India. A commercial HIPOJET-2100 device was used for the spraying procedure. Before the coatings were applied, the samples underwent alumina powder grit blasting. Approximately 250 μm thick coatings were applied. Table 2 displays the process parameters of the HVOF spraying method. These process parameters were maintained throughout the spraying procedure.

Table 2. HVOF spraying process parameters

Oxygen flow rate	300 L min ⁻¹
Fuel (acetylene) flow rate	120 L min ⁻¹
Air-flow rate	600 L min ⁻¹
Spray distance	200 mm
Powder feed rate	25 g min ⁻¹
Fuel pressure	1.8 kg cm ⁻²
Oxygen pressure	2.90 kg cm ⁻²
Air pressure	4.00 kg cm ⁻²

Evaluation of coating properties

During the spraying process, the thickness of each coating was measured using a Minitest-2000 thin film thickness gauge (Elektro-Physik Koln Company, Germany, precision $\pm 1 \mu\text{m}$). Prior to porosity measurement, the specimens were polished. The computer-based porosity analysis technology turns the pore regions (gray-level areas) into a background colour that differs from the rest of the microstructure in order to calculate the pore area size. The porosity value is then determined by the computer system by counting the number of background colour pixels. For every type of coated specimen, the mean of five porosity measurements was determined. The surface roughness of the coated samples was measured with the help of a surface roughness tester (Surftest SJ310, Mitutoyo) and average surface roughness (R_a) values were recorded. For the measurements of microhardness, a digital micro Vickers hardness tester (SHV-1000, Chennai Metco Private Limited, Chennai) was used. The microhardness was measured along the cross section at fixed intervals on the coating–substrate interface.

Hot corrosion investigations

Prior to being subjected to high-temperature corrosion studies in a molten salt environment, each sample underwent wheel polishing. Using a camel hair brush, samples heated to 250 °C were coated with molten salt (Na_2SO_4 -60 % V_2O_5) and achieved a consistent thickness of 3 to 5 mg cm⁻². Hot corrosion investigations were then conducted under cyclic circumstances involving 50 cycles. Every experimental cycle comprised an hour of exposure at 850 °C in a tube boiler, succeeded by a 20-minute cooling period at room temperature. Every sample was exposed to a heated corrosion environment while placed on a separate alumina boat. The cyclic studies were conducted to replicate the real boiler environment, and it has been found that 50 cycles of experimentation are

sufficient to achieve steady-state corrosion of the alloy. At the end of each cycle, weight was recorded using an electronic balance with a minimum count of 1 mg. In order to compute mass gain, the spalled oxide scale was also used in the weight measurements. To approximate the kinetics of high temperature corrosion in a chosen environment, weight gain data was studied. Following their exposure to hot corrosion, the corroded samples underwent cross-sectional examination using XRD, SEM, and EDAX techniques.

Results

Coating thickness, porosity, surface roughness and bond strength measurement

During the spraying process, the thickness of each coating was measured using a Minitest-2000 thin film thickness gauge and the results are displayed in Table 3. The coating thickness was measured along the specimen cross-sections, and it was discovered to be within the intended range. Since the thermal spray coatings are porous by nature, porosity has a significant impact on the coating characteristics. The literature reveals that coatings with less porosity provide superior corrosion protection [5,8]. The apparent porosity measurements of the T22 steel specimens coated with Cr₂O₃ and Cr₂O₃-5 wt.% YSZ are presented in Table 3. For every sample, the porosity readings of the Cr₂O₃ coating sprayed with HVOF were less than 2 %. The porosity value continues to decrease with the increase of YSZ content, according to the values given in the table. The nano YSZ was able to fill the macro pores in conventional chromium oxide powder, which resulted in a reduction of porosity. The porosity values for HVOF-sprayed Cr₂O₃ coatings are comparable to those documented in the literature [9]. The surface roughness values for the Cr₂O₃ and 5 wt.% YSZ reinforced Cr₂O₃ nanocomposite coated samples were found to be 3.15 and 2.53 μm, respectively. The porosity and surface roughness of thermal spray coatings influence each other. A low value of porosity helps to reduce surface roughness, which in turn enhances the microhardness of coatings. A higher microhardness helps to increase the corrosion resistance of coatings. The bond strength of developed coatings was measured by peel-off test, and bond strength values are given in Table 3.

Table 3. Average coating thickness and porosity values for different coatings on ASME-SA213-T22

Coating	Coating thickness, μm	Porosity, %	Average surface roughness, μm	Bond strength, MPa
Cr ₂ O ₃	255	1.91	3.83	73
Cr ₂ O ₃ -5 wt.% YSZ	257	1.73	3.09	77

Microhardness measurement

Figure 1 displays the microhardness characteristics for both coated specimens over their cross-section. T22 steel had microhardness values between 258 and 288 HV. The Cr₂O₃ and Cr₂O₃-5 wt.% YSZ coated specimens had microhardness readings in the following ranges: 1236 to 1276 and 1346 to 1386 HV, respectively. Figure 1 shows that the micro-hardness value rises with the addition of YSZ in the chromium oxide matrix. The microhardness of Cr₂O₃ coatings sprayed by HVOF was enhanced by the YSZ. The microhardness profiles distinctly demonstrate that all coated specimens were found to have approximately consistent hardness throughout the coating cross-section.

Hot corrosion experimentation

Figure 2 displays the weight change curves for the uncoated, Cr₂O₃ coated, and Cr₂O₃-5 wt.% YSZ nanocomposite-coated T22 steel samples after exposure to high-temperature corrosion. The weight gain for the hot corrosion of uncoated T22 steel at 900 °C began during the first cycle of the investigation and increased steadily until the end of 50 cycles.

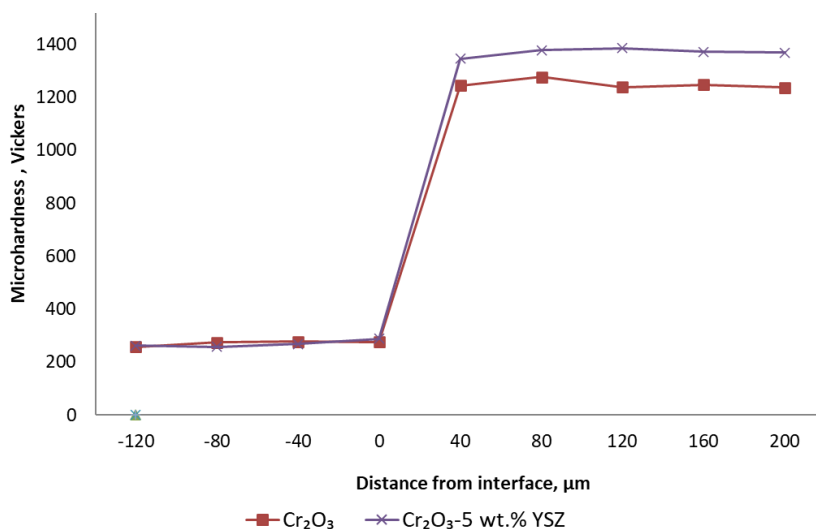


Figure 1. Microhardness profiles of nanocomposite coatings across the cross-section

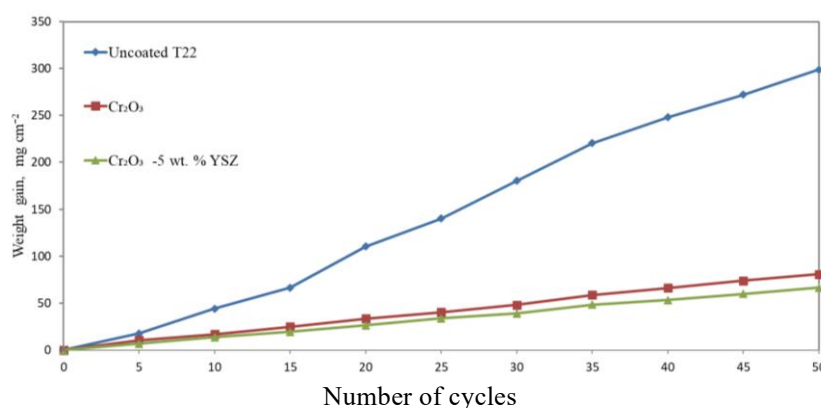


Figure 2. Weight gain/area vs. time (number of cycles) of hot corrosion for uncoated, Cr_2O_3 coated, and Cr_2O_3 -5 wt.% YSZ coated T22 steel

Weight gain plots indicated that Cr_2O_3 and YSZ-reinforced Cr_2O_3 coatings on T22 steel are significantly protected against hot corrosion in molten salt at 900 °C. When compared to uncoated steel, the rate of weight gain for Cr_2O_3 -coated steel is significantly lower. As shown in Figure 2, the inclusion of YSZ in the Cr_2O_3 coating enhanced the resistance to corrosion of T22 steel and decreased its cumulative weight increase following 50 cycles of hot corrosion at 900 °C. Thus, in a molten salt environment at 900 °C, it was discovered that the Cr_2O_3 -5 wt.% YSZ coating on T22 steel has the lowest rate of weight gain during high-temperature corrosion.

Figure 3 displays the nature of fit for high-temperature corrosion at 900 °C for all samples, plotting $(\text{weight gain/area})^2$ vs. number of cycles (50 cycles). Whereas the Cr_2O_3 and YSZ reinforced Cr_2O_3 coated T22 steel samples followed the parabolic rate law, the untreated T22 steel showed slight divergence. The slope of the fitted linear regression line yields the parabolic rate constant (K_p). Table 5 displays K_p values and the total weight gain following exposure. It was discovered that the K_p values for the coated T22 samples were substantially lower than those for the uncoated T22 steel sample. On T22 steel, the Cr_2O_3 -5 wt.% YSZ coating has the lowest K_p value.

Table 5. Parabolic rate constant and cumulative weight gain for all samples

Type of coating	$K_p / 10^{-10} \text{ g}^2 \text{ cm}^{-4} \text{ s}^{-1}$	Total weight (cumulative) gain, mg cm^{-2}
Uncoated T22 steel	4964.06	298.92
Cr_2O_3	361.62	80.68
Cr_2O_3 -5 wt.% YSZ	245.38	66.46

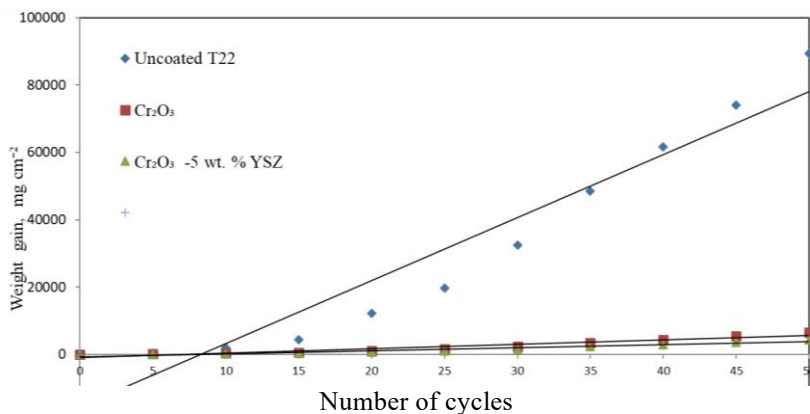


Figure 3. (Weight gain/area)² vs. number of cycles (50 cycles) of hot corrosion for uncoated, Cr₂O₃ coated, and Cr₂O₃-5 wt.% YSZ coated T22 steel

FE-SEM/Energy dispersive X-ray spectroscopy analysis

Figure 4 displays the EDAX analysis and FE-SEM micrographs of all samples following hot corrosion in a Na₂SO₄ – 60 % V₂O₅ atmosphere for 50 cycles at 900 °C.

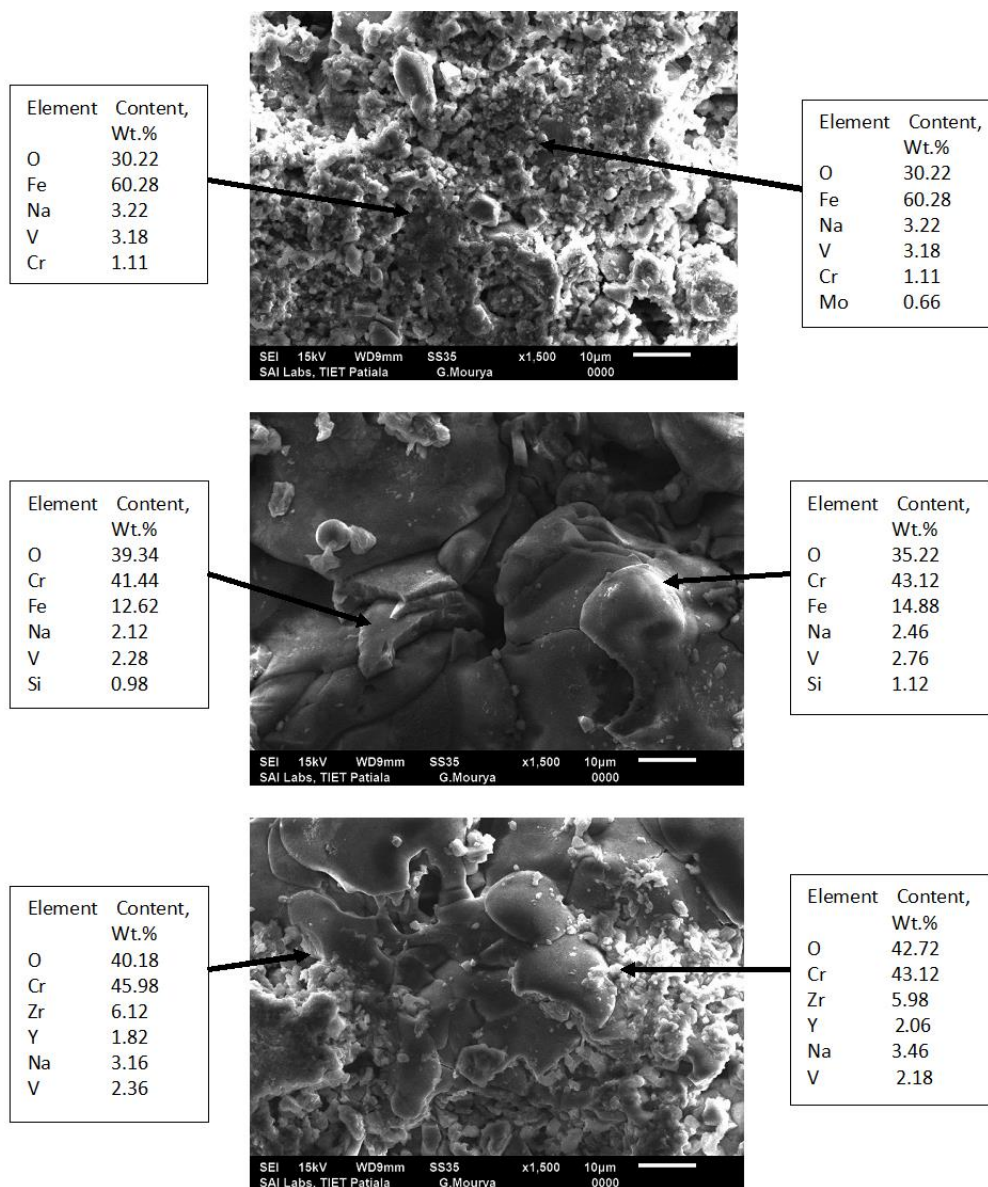


Figure 4. FE-SEM with EDS analysis of HVOF sprayed coatings: (a) uncoated T22, (b) Cr₂O₃, (c) Cr₂O₃-5 wt.% YSZ coated T22 steel samples after hot corrosion at 900 °C

Uncoated T22 steel corroded at 900 °C (Figure 4a) appears to have irregularly shaped flakes randomly orientated in the oxide scale. There are white areas and a porous appearance to the oxide scale. Rich concentrations of Fe and O were found in the oxide scale at a few chosen places in the EDAX analysis, in addition to a notable presence of Na, V, and Cr. In a few different places, the presence of Mo is also somewhat visible. According to EDAX compositions, there is a high likelihood that Fe, Cr, Mo, and Na oxides will form in the scale, with iron oxide being the predominant phase. The microscopy of Cr₂O₃-coated T22 steel (Figure 4b) shows that the scale was composed of nodules after exposure to 900 °C. The EDAX analysis at points 1 and 2 showed that Cr and O made up the majority of the scale. While the presence of Na and V indicated the presence of molten salt components in the scale, the presence of Fe and Si may be the result of these elements diffusing from the substrate to the coating matrix at 900 °C. The micrograph of Cr₂O₃-5 wt.% YSZ coated T22 steel (Figure 4c) indicates a significant amount of Cr and O with small amounts of Y, Zr, Na and V in the scale composition. Rich Cr and O presences were found in all examined locations, coupled with a high presence of Zr and Y, according to the EDAX analysis. Zr and Y were found in the oxide scale even after hot corrosion at 900 °C. Additionally, trace amounts of Na and V showed that following intense corrosion at 900 °C, molten salt components are present in the oxide scale.

Discussion

In this research work, Cr₂O₃ coated and Cr₂O₃-5 wt.% YSZ nanocomposite coatings were successfully developed on T22 steel using the HVOF spraying method. The thickness of both coatings was equal to 255 and 257 μm, respectively. The same range of thickness of HVOF sprayed coatings has been reported by various authors [10,16-18]. The porosity of conventional Cr₂O₃ coating on T22 boiler tube steel was found to be 1.91 %, which is reduced to 1.73 % with the addition of 5 wt.% YSZ in Cr₂O₃ matrix. The addition of YSZ reduced the porosity of the Cr₂O₃ coating by 9.42 %. This might be due to the filling of micropores in Cr₂O₃ coating by nanoparticles of YSZ. The reduction in porosity also improved the surface roughness value of YSZ-reinforced Cr₂O₃ coating. The surface roughness values for the Cr₂O₃ and 5 wt.% YSZ reinforced Cr₂O₃ nanocomposite coated samples were found to be 3.83 μm and 3.09 μm, respectively. Goyal and Goyal [19] have reported a decrease in the porosity of thermal sprayed coatings with the addition of carbon nanotubes. Microhardness values of Cr₂O₃ and 5 wt.% YSZ reinforced Cr₂O₃ nanocomposite coated samples were found to be in the range of 1236-1276 HV and 1346-1386 HV, respectively. The addition of nano YSZ in the Cr₂O₃ matrix has led to an increase in the microhardness of the coating. Indentation resistance was increased by adding nanoparticles to the coating matrix. Strong heat conductivity of YSZ could lead to more melting, which raises the microhardness of coatings reinforced with YSZ. The porosity of the Cr₂O₃ matrix decreased due to the nano YSZ particles filling the coating matrix pores and dispersing evenly throughout. Dispersion hardening or a decrease in the porosity of the coating matrix may be the cause of the hardness increase [9].

When the uncoated T22 steel was exposed to the molten salt atmosphere at 900 °C for 50 cycles, there was significant spalling and sputtering of the oxide scale. Similar types of oxide scale spallation for boiler tube steels during high-temperature corrosion studies in similar environments have also been described by Sidhu *et al.* [20]. The Cr₂O₃ and YSZ reinforced Cr₂O₃ coated steel showed comparatively less weight gain, suggesting that these coatings offered adequate protection against hot corrosion. The cumulative weight gain of the uncoated T22 boiler steel specimen was found to be 298 mg cm⁻², whereas the cumulative weight gain of Cr₂O₃ and YSZ reinforced Cr₂O₃ coated steel specimens was found to be 80.68 and 66.46 mg cm⁻², respectively. The Cr₂O₃ on T22 steel was able

to reduce the weight gain of uncoated steel by 73 % and the addition of nano YSZ particles in Cr₂O₃ coating further reduced the weight gain to 77.76 %. Otsuka and Rapp [21] and Ozgurluk *et al.* [3] have also observed higher weight gain for boiler steels in identical molten salt environments. The microstructural study of uncoated steel indicated the formation of a weak, non-protective Fe₂O₃ scale with cracks. At specific points, SEM/EDAX investigation verified the production of Fe₂O₃. Fe and O elements were also detected in the oxide scale by the cross-sectional EDAX analysis, confirming the production of Fe₂O₃. It is possible that the precipitation of Fe₂O₃ from the liquid phase during the thermal cycle cooling phase led to severe strain and scale spalling and cracks that might have allowed the molten components to seep into the steel substrate. In high-temperature corrosion experiments, El-Awadi *et al.* [22] found that the Fe₂O₃ scale is not protective. Mo may generate an inner layer of MoO₃ at the substrate scale contact due to the presence of Mo in the substrate steel; this liquid oxide fractures and dissolves the protective oxide scale, accelerating corrosion [23,24].

HVOF sprayed Cr₂O₃ coating on T22 steel was able to decrease the corrosion rate by 73 % after hot corrosion at 900 °C. EDAX measurements have verified the presence of Fe at certain locations (Figure 4(b)). Fe may have penetrated through the pores in the Cr₂O₃ coating matrix. Si might have further increased the strain on the oxide scale in the EDAX analysis (Figure 4(b)), which would have caused the scale of the Cr₂O₃-coated T22 steel sample to crack. Karaoglalini *et al.* [24] reported that hot corrosion salts leaked from the gaps and pores as in the coating system and formed reactions with Al, Mg, Si, and Ca elements in the coating. Weight gain plots indicated that protection from hot corrosion at 900 °C in a molten salt environment has been provided by nano YSZ reinforced chromium oxide coatings on T22 steel. The YSZ- Cr₂O₃ coatings were intact, without cracks and spallation, after 50 cycles of studies. Kumar *et al.* [25] have also reported that CNT-based reinforced coatings showed lower weight gain along with the formation of protective oxide scales during the experimentation. Improvement in protection against hot corrosion was observed with an increase in CNT content in the coating matrix. The cumulative weight gain/unit area for Cr₂O₃-5 wt.% YSZ coated T22 steel after hot corrosion at 900 °C for 50 cycles was found to be 66.46 mg cm⁻². Additionally, the parabolic law has been followed by the YSZ-reinforced chromium oxide-coated steel, indicating that the produced scales have a tendency to act as diffusion barriers to corrosive species. The values of parabolic rate constant (K_p) for YSZ reinforced coatings were found to be significantly lower than uncoated T22 and Cr₂O₃ coated T22. The minimum value of K_p was observed for Cr₂O₃-5 wt.% YSZ coating on T22 steel ($245.38 \times 10^{-10} \text{g}^2 \text{cm}^{-4} \text{s}^{-1}$), and this coating showed higher corrosion resistance than all other coatings in the molten salt environment at 900 °C for 50 cycles. The presence of YSZ and the development of a protective chromium oxide scale during hot corrosion at 900 °C have been attributed to the much higher corrosion protection offered by YSZ-reinforced coatings; the presence of Zr and Y have also been confirmed in EDAX analysis at specific places. By limiting the penetration of corroding elements, the YSZ was able to reduce the porosity of YSZ-reinforced coatings, thus enhancing their ability to withstand corrosion at 900 °C.

Conclusions

The following conclusions are made from this experimental work:

- In this research work, the hot corrosion behaviour of Cr₂O₃ coated and Cr₂O₃-5 wt.% YSZ coatings on T22 steel was investigated at 900 °C in a molten salt environment.
- The thickness of HVOF sprayed Cr₂O₃ and Cr₂O₃-5 wt.% YSZ nanocomposite coatings was found to be in the range of 250-260 μm.

- With the addition of YSZ particles in nanocomposite coating, the porosity value decreases. The Cr₂O₃-5 wt.% YSZ coating was found to have the lowest porosity value of 1.73 %. A decrease in porosity resulted in an improvement in surface roughness values and an increase in microhardness values.
- The formation of protective chromium oxides allowed the Cr₂O₃ coated steel to effectively reduce weight increase by 73 % compared to uncoated T22 steel.
- The Cr₂O₃-5 wt.% YSZ nanocomposite coating was able to enhance corrosion resistance due to the addition of YSZ nanoparticles. 5 wt.% YSZ reinforced coating on steel reduced the cumulative weight gain of uncoated T22 steel by 77.76 %.

Acknowledgements: This research received no specific grant from any funding agency in the public, commercial, or not-for-profit sectors.

Conflict of interest: The authors also declare that they have no conflict of interest.

References

- [1] J. Lehmusto, D. Lindberg, P. Yrjas, L. Hupa, The Effect of Temperature on the Formation of Oxide Scales Regarding Commercial Superheater Steels, *Oxidation of Metals* **89** (2018) 251-278. <https://doi.org/10.1007/s11085-017-9785-6>
- [2] A. Keyvani, M. Bahamirian, Hot corrosion and mechanical properties of nanostructured Al₂O₃/CSZ composite TBCs, *Surface Engineering* **33** (2017) 433-443. <https://doi.org/10.1080/02670844.2016.1267423>
- [3] Y. Ozgurluk, K. M. Doleker, A. C. Karaoglanli, Hot corrosion behavior of YSZ, Gd₂Zr₂O₇ and YSZ/Gd₂Zr₂O₇ thermal barrier coatings exposed to molten sulfate and vanadate salt, *Applied Surface Science* **438** (2017) 96-113. <https://doi.org/10.1016/j.apsusc.2017.09.047>
- [4] B. S. Sidhu S. Prakash, Erosion-corrosion of plasma as sprayed and laser remelted Stellite-6 coatings in a coal fired boiler, *Wear* **260** (2006) 1035-1044. <https://doi.org/10.1016/j.wear.2005.07.003>
- [5] T. Sidhu, S. Prakash, R. Agrawal, Hot corrosion studies of HVOF sprayed Cr₃C₂-NiCr and Ni-20Cr coatings on nickel-based superalloy at 900 °C, *Surface and Coatings Technology* **201** (2006) 792-800. <https://doi.org/10.1016/j.surfcoat.2005.12.030>
- [6] T. Sidhu, S. Prakash, R. Agrawal, Study of Molten Salt Corrosion of Superni-75 using Thermo-gravimetric Technique, *Journal of Naval Architecture and Marine Engineering* **3** (2006) 77-82. <https://citeseerx.ist.psu.edu/document?repid=rep1&type=pdf&doi=973e1d73faf05a362486009ae39c760fcdadcdf1>
- [7] B.K. Bhagria, D. Mudgal, S.S. Sidhu, R. Verma, Present scenario of hot corrosion studies performed with ferritic steel, *AIP Conference Proceedings* **2341(1)** (2021) 040034. <https://doi.org/10.1063/5.0049955>
- [8] B. S. Sidhu, Prakash, S., Nickel-chromium plasma spray coatings: A way to enhance degradation resistance of boiler tube steels in boiler environment. *Journal of Thermal Spray Technology* **15** (2006) 131-140. <https://doi.org/10.1361/105996306X92695>
- [9] K. Goyal, H. Singh, R. Bhatia, Effect of Carbon Nanotubes on Properties of Ceramics Based Composite Coatings, *Advanced Engineering Forum* **26** (2018) 53-66. <https://doi.org/10.4028/www.scientific.net/AEF.26.53>
- [10] M. Kuruba, G. Gaikwad, D. Shivalingappa, Hot-corrosion behaviour of CNT reinforced Cr₃C₂-NiCr coatings working under high-temperature sprayed by HVOF method, *Proceedings of the Institution of Mechanical Engineers, Part L: Journal of Materials: Design and Applications* **236(12)** (2022) 2372-2383. <https://doi.org/10.1177/14644207221082237>
- [11] S. Singh, K. Goyal, R. Bhatia, Mechanical and microstructural properties of yttria-stabilized zirconia reinforced Cr₃C₂-25NiCr thermal spray coatings on steel alloy, *Journal of*

Electrochemical Science and Engineering **12(5)** (2022) 819-828.

<https://doi.org/10.5599/jese.1278>

- [12] S. Singh, K. Goyal, R. Bhatia, Effect of nano yttria-stabilized zirconia on properties of Ni-20Cr composite coatings, *Journal of Electrochemical Science and Engineering* **12(5)** (2022) 901-909. <https://doi.org/10.5599/jese.1319>
- [13] D. K. Goyal, H. Singh, H. Kumar, V. Sahni, Slurry erosion behaviour of HVOF sprayed WC–10Co–4Cr and Al₂O₃+ 13TiO₂ coatings on a turbine steel, *Wear* **289** (2012) 46-57. <https://doi.org/10.1016/j.wear.2012.04.016>
- [14] K. Goyal, V.P.S. Sidhu, R. Goyal, Hot Corrosion Study of High Velocity Oxyfuel (HVOF) Sprayed Coatings on Boiler Tube Steel in Actual Coal Fired Boiler, *Pakistan Journal of Scientific & Industrial Research Series A: Physical Sciences* **61** (2018) 149-155. <https://v3.pjsir.org/index.php/physical-sciences/article/view/307>
- [15] Sahil, S. Singh, K. Goyal, D. Bhandari, B. Krishan, Hot corrosion behaviour of thermal-sprayed TiO₂-reinforced Cr₂O₃ composite coatings on T-22 boiler steel at elevated temperature, *Journal of Bio-and Tribo-Corrosion* **7(3)** (2021) 100. <https://doi.org/10.1007/s40735-021-00536-1>
- [16] M. Shi, Z. Xue, H. Liang, Z. Yan, X. Liu, S. Zhang, High velocity oxygen fuel sprayed Cr₃C₂-NiCr coatings against Na₂SO₄ hot corrosion at different temperatures, *Ceramics International* **46** (2020) 23629-23635. <https://doi.org/10.1016/j.ceramint.2020.06.135>
- [17] S. Muthu, M. Arivarasu, Investigations of hot corrosion resistance of HVOF coated Fe based superalloy A-286 in simulated gas turbine environment, *Engineering Failure Analysis* **107** (2020) 104224. <https://doi.org/10.1016/j.engfailanal.2019.104224>
- [18] N. Abu-warda, A. López, M. López, M. Utrilla, Ni20Cr coating on T24 steel pipes by HVOF thermal spray for high temperature protection, *Surface and Coatings Technology* **381** (2020) 125133. <https://doi.org/10.1016/j.surfcoat.2019.125133>
- [19] K. Goyal, R. Goyal, Improving hot corrosion resistance of Cr₃C₂-20NiCr coatings with CNT reinforcements, *Surface Engineering* **36** (2019) 1200-1209. <https://doi.org/10.1080/02670844.2019.1662645>
- [20] V. P. Singh Sidhu, K. Goyal, R. Goyal, Corrosion behaviour of HVOF sprayed coatings on ASME SA213 T22 boiler steel in an actual boiler environment, *Advanced Engineering Forum* **20** (2017) 1-9. <https://doi.org/10.4028/www.scientific.net/AEF.20.1>
- [21] N. Otsuka, R. A. Rapp, Hot Corrosion of Preoxidized Ni by a Thin Fused Na₂SO₄ Film at 900 °C, *Journal of The Electrochemical Society* **137** (1990) 46-52. <https://doi.org/10.1149/1.2086436>
- [22] G. El-Awadi, S. Abdel-Samad, E. S. Elshazly, Hot corrosion behavior of Ni based Inconel 617 and Inconel 738 superalloys, *Applied Surface Science* **378** (2016) 224-230. <https://doi.org/10.1016/j.apsusc.2016.03.181>
- [23] R. Goyal, K. Goyal, Development of CNT reinforced Al₂O₃-TiO₂ coatings for boiler tubes to improve hot corrosion resistance, *Journal of Electrochemical Science and Engineering* **12(5)** (2022) 937-945. <https://doi.org/10.5599/jese.1291>
- [24] A. C. Karaoglanli, Y. Ozgurluk, A. Gulec, D. Ozkan, G. Binal, Effect of coating degradation on the hot corrosion behavior of yttria-stabilized zirconia (YSZ) and blast furnace slag (BFS) coatings, *Surface and Coatings Technology* **473** (2023) 130000. <https://doi.org/10.1016/j.surfcoat.2023.130000>
- [25] S. Kumar, R. Bhatia, H. Singh, Hot corrosion behaviour of CNT-reinforced ZrO₂-Y₂O₃ composite coatings on boiler tube steel at 900 °C, *Anti-Corrosion Methods and Materials* **68(6)** (2021) 503-515. <https://doi.org/10.1108/ACMM-12-2020-2412>